Eur. Phys. J. B (2014) 87: 236
DOI: 10.1140/epjb/e2014-50322-y

THE EUROPEAN PHYSICAL JOURNAL B

Regular Article

Perceptron-like computation based on biologically-inspired neurons with heterosynaptic mechanisms

Pablo Kaluza[1,2,a] and Eugenio Urdapilleta[3]

[1] Instituto de Ciencias Básicas, Universidad Nacional de Cuyo. Padre Contreras 1300, 5500 Mendoza, Argentina
[2] Consejo Nacional de Investigaciones Científicas y Técnicas, Buenos Aires, Argentina
[3] División de Física Estadística e Interdisciplinaria, Centro Atómico Bariloche, Av. E. Bustillo Km 9.500, S.C. de Bariloche, 8400 Río Negro, Argentina

Received 19 May 2014 / Received in final form 22 August 2014
Published online 20 October 2014 – © EDP Sciences, Società Italiana di Fisica, Springer-Verlag 2014

Abstract. Perceptrons are one of the fundamental paradigms in artificial neural networks and a key processing scheme in supervised classification tasks. However, the algorithm they provide is given in terms of unrealistically simple processing units and connections and therefore, its implementation in real neural networks is hard to be fulfilled. In this work, we present a neural circuit able to perform perceptron's computation based on realistic models of neurons and synapses. The model uses Wang-Buzsáki neurons with coupling provided by axodendritic and axoaxonic synapses (heterosynapsis). The main characteristics of the feedforward perceptron operation are conserved, which allows to combine both approaches: whereas the classical artificial system can be used to learn a particular problem, its solution can be directly implemented in this neural circuit. As a result, we propose a biologically-inspired system able to work appropriately in a wide range of frequencies and system parameters, while keeping robust to noise and error.

1 Introduction

Artificial neural networks have shown to be a powerful tool to theoretically understand the basic functionality principles of neural biological systems and, in particular, neural computation. The perceptron model [1], with its associated backpropagation algorithm for learning [2], and the Hopfield model of associative memory [3] are fundamental and paradigmatic building blocks in this field. One of the strengths of these models is the use of simplified descriptions for neurons, synapses, structure and dynamics. These simplifications allow modelers to apply different methods to disentangle the roots of the computational power they achieve and to use these models for particular computational tasks [4].

On the other hand, detailed models of biological neural components, including the classical model of neuronal excitability due to Hodgkin and Huxley [5], are focused on the precise description of the biophysical aspects of neurons and synapses. These models are relevant to analyze delicate aspects of neural systems dynamics and their influence on cognitive function; for example, synchronization and oscillatory properties [6,7], stimuli encoding as different spiking sequences [8], and the diverse characteristic firing behaviors across neurons [9], to name a few. However, these studies are generally not oriented to study the computational properties that emerge from a connectionism point of view.

The construction of artificial neural networks with elements based on more realistic descriptions has been the natural continuation in the field, aimed to understand the computational abilities of real neural systems [10]. In this direction, Hopfield-like models with phase oscillators as processing units [11], instead of spins, have been extensively studied [12–15]. Moreover, the use of oscillators as computing elements in feedforward perceptron networks has been also considered by one of the authors [16]. Current efforts also include the elucidation of the link between those foundational processes in artificial neural networks research and their counterparts in biologically realistic spiking networks; for example, the learning rule in feedforward networks has been analyzed in spiking networks with simple or detailed physiological descriptions [17,18].

In this work, we extend previous studies on biologically inspired feedforward networks with computational capacities. In particular, we assume that a perceptron has evolved by learning and, by a proper design of computing elements and connections, we construct a biologically realistic neural system on top of which classical perceptron can be expressed. The biological realism of this system must be seen in terms of synthetic biology [19] and not as a description of a real system. This work continues one of the author's previous theoretical study on perceptrons made by phase oscillators [16] and, as before, it is aimed

[a] e-mail: pkaluza@mendoza-conicet.gob.ar

to resolve a computational task (e.g., classification), now with neurophysiologically-based dynamical properties. We use realistic models of neurons and synapses, and combine them in a proper network architecture to construct the computational function. As a result, we explicitly obtain a spiking neural system able to work with the weights, thresholds and main architecture of a classical perceptron feedforward network. As an extension of the perceptron, this model naturally is capable to solve binary settings, and adds functionality regarding operation at different frequencies and noise levels.

The work is organized as follows. In the second section we present the spiking perceptron model and the interconnection between processing units. In the third section we carry out a detailed numerical study of this model and its operation, construct a feedforward network capable to solve the XOR logic problem, and describe its extension to any perceptron processing scheme. Finally, in the last section we discuss about our findings and present our concluding remarks.

2 Model

We propose a model in which the information is encoded as the neural activity on a binary basis. Under this definition, the neuron is active if it is spiking; otherwise, it is inactive. Activation indicates that a neuron is spiking with a mean frequency similar to that of some reference neuron. When its frequency is much smaller (e.g. an order of magnitude less than the frequency of the reference neuron), the neuron is considered inactive.

All neurons in the network evolve according to a conductance-based neural dynamics, similar to the Hodkgin-Huxley model. In particular, the neuron model we use has been proposed by Wang and Buzsáki to describe the intrinsic neural dynamics in a hippocampal network and, as detailed in the Appendix, it is based on two gating dynamics relative to spike-initiation currents [20]. This neuron model has been extensively used, for example, to study synchronization properties of inhibitory or inhibitory/excitatory populations of neurons [20–22], the generation of rhythms in hippocampal networks [23,24], the modulation of synchrony by competition in recurrent networks and its influence on attentional response functions [25,26], stimuli encoding in neuron models [27], to name a few studies. Regarding its encoding capabilities [27], this model corresponds to a type I neuron class and presents a saddle-node bifurcation with respect to the input current, in contrast to the Hodgkin-Huxley model which presents a Hopf bifurcation from quiescent to spiking regime and, therefore, it is classified as a type II neuron. We selected this model in order to avoid bistability with respect to the input current, and then, to directly extend the results and be compatible with our previous theoretical model [16]. Moreover, we present a detailed analysis of our election in the numerical study section.

Hereafter, the elemental unit in our model is called the processing unit and it consists of a circuit of two neurons, as shown in Figure 1a. This irreducible unit has a

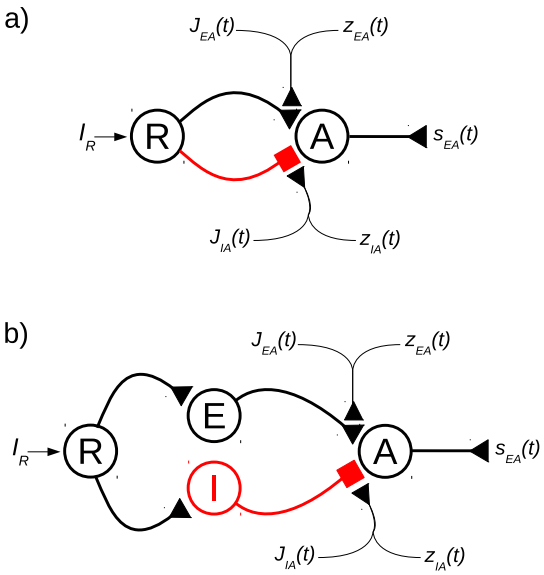

Fig. 1. (a) Neural circuit as spiking perceptron. This circuit comprises a processing neuron A and a reference neuron R. They are connected by two chemical synapses, one inhibitory (red square arrow) and one excitatory (black triangular arrow). The efficiency of these synapses, or weight, is modulated by input signals provided by the neural network, $z_{IA}(t)$ and $z_{EA}(t)$, and external inputs, $J_{IA}(t)$ and $J_{EA}(t)$, through excitatory axo-axonic heterosynapsis. The reference neuron R has an independent input current I_R that regulates its activity. The output signal of the processing neuron has a postsynaptic effect characterized by the function $s_{EA}(t)$. (b) Equivalent circuit where neurons have only one type of output synapse. In this case, neuron R is exclusively excitatory, and connects to an inhibitory neuron I (red square arrow) and an excitatory neuron E (black triangular arrow).

processing neuron A and a reference neuron R; whereas neuron A is independent for each unit, neuron R may be shared among them (but not limited to) and therefore be a global reference. These neurons are connected from R to A by two chemical synapses with opposite effects, one inhibitory and one excitatory. The distinctive feature of this processing unit is that while it is synaptically and exclusively driven by the reference neuron, it also processes signals coming from either other neurons' outputs, $z_{\alpha A}(t)$, or external sources, $J_{\alpha A}(t)$, by modulating the efficiency of the synapses (note the subindex *alpha* in the signals, representing the modulation to either an excitatory or an inhibitory synapse, $\alpha = E, I$, respectively) via an axo-axonic heterosynaptic synaptic mechanism. This kind of synaptic mechanism is well known in neural systems [28–32], as it modulates the pre/post synaptic function by a third participant (heterosynapsis) and is involved in fast neural processing (electrical axo-axonic coupling). Additionally, this concerted mechanism has been conceptually used in artificial neural networks with high-order connections [33,34]. As discriminated in the notation, the signals to be processed are generally time-dependent and are originated from two sources: by the activity of other neurons in the system, via $z_{\alpha A}(t)$, or from external inputs,

through $J_{\alpha A}(t)$. For the sake of simplicity, we consider that these input signals only excite those synapses they impinge on. Thus, $z_{IA}(t)$ and $J_{IA}(t)$ facilitate the corresponding inhibitory synapse, whereas $z_{EA}(t)$ and $J_{EA}(t)$ facilitate the excitatory one.

The reference neuron R fires periodically with a frequency ν_R, fixed by the input current I_R. This neuron has two output synapses, one excitatory and one inhibitory. Although this kind of dual behavior is not habitual in real neurons, we can consider this circuit as a minimum effective representation. In effect, as shown in Figure 1b, an equivalent circuit can be obtained with all neurons presenting a single synaptic behavior. The operation of these two circuits is essentially equivalent, except for delays not considered in this work.

The total input current I_A arriving to the processing neuron A is given by the summation of the synaptic input currents I_{EA} (excitatory) and I_{IA} (inhibitory). Synaptic currents are modelled as conductance-based descriptions [22], with a maximal conductance given by the modulation in the axo-axonic connection; in detail,

$$I_{\alpha A} = G_\alpha\big(z_{\alpha A}(t), J_{\alpha A}(t)\big)\ (V_\alpha - V_A)\ s_{\alpha R}(t). \qquad (1)$$

In this expression, V_A is the potential of the postsynaptic neuron A and V_α is the reverse potential of the synapse under analysis, given by $\alpha = I, E$ (inhibitory and excitatory, respectively). Numerical values of the parameters and model details are given in the Appendix. The function $s_{\alpha R}(t)$ is the signal coming from the presynaptic neuron R and it is commonly modelled as the difference of two exponential functions with different time constants (see Appendix for details). In contrast with traditional models and following our previous work (see Ref. [16]), the weight of the synapse $G_\alpha(z_{\alpha A}(t), J_{\alpha A}(t))$ is a function of the incoming signal $z_{\alpha A}(t)$ (from other processing units) and $J_{\alpha A}(t)$ (from an external source). This mechanism corresponds to an axo-axonic synapse and it is a key feature in our work. We consider these two signals as separate streams only for the sake of clarity since, in effect, both inputs have the same nature. The function of the signal $J_{\alpha A}(t)$ is to bring information to the system (neural network) from the outside environment.

The input signal $z_{\alpha A}(t)$ due to the activity of other nodes of the system is collected by a processing unit A as the summation of m_{EA} excitatory and m_{IA} inhibitory output signals generated by those connected preceding units. Since the output signal of a processing unit, $R+A$, is that signal generated by its processing neuron A, we use the same index to refer to the processing unit or, indistinctively, to its corresponding processing neuron. Each signal is given by:

$$z_{\alpha A}(t) = \sum_{j=1}^{m_{\alpha A}} w_{Aj}^{\alpha} s_{Ej}(t). \qquad (2)$$

In this expression, the constant w_{ij}^{α} weights the modulation of the axo-axonic synapse of kind α, due to the unit j, on the synapse between the neuron A and its reference neuron R. The function $s_{Ej}(t)$ is the postsynaptic excitatory signal generated by the preceding neuron j. Finally, we define

$$G_\alpha\big(z_{\alpha A}(t), J_{\alpha A}(t)\big) = W\ g_\alpha z_{\alpha_A}(t) + J_{\alpha_A}(t), \qquad (3)$$

where the constants g_α are factors added to compensate excitatory and inhibitory effects, and the constant W is an amplification factor valid for all input neural signals. Note that the weight function $G_\alpha(z_{\alpha A}(t), J_{\alpha A}(t))$ must return values with units of mS/cm^2. However, for the sake of clarity, we consider all input signals and factors as dimensionless. The correct units can be achieved by a multiplicative unitary factor with the proper units.

3 Numerical study

In this section we numerically study the main properties of this model and construct an explicit example of a feedforward network able to solve the XOR logic problem with the proposed processing units. All numerical simulations are carried out using a Runge-Kutta integration algorithm of second order with $\Delta t = 0.01$ ms. Unless otherwise specified, the spiking frequency of any neuron is defined as the inverse of the interspike intervals observed during a 10 000 ms window.

3.1 Spiking perceptron versus classical perceptron

In order to study the relationship between the classical perceptron model and the proposed model for an equivalent spiking perceptron, we firstly study the response of the processing unit with respect to constant external signals $J_{\alpha A}$, neglecting any other input activity from other processing units ($z_{\alpha A}(t) = 0$).

To that purpose, we consider the processing unit illustrated in Figure 1a with $I_R = 1$ mA/cm^2. Driven by this stimulation, the reference neuron fires with a constant frequency of $\nu_R \approx 60$ Hz. In Figure 2a we present the frequency of the processing neuron ν_A as a function of the external input signal J_{EA}. The figure shows several curves corresponding to different values J_{IA} of a simultaneous inhibition. According to equation (3), the synapse between R and A is being strongly modulated by input signals and therefore, the processing unit needs an external signal $J_{EA} \neq 0$ to present some activity and start to spike. This behavior is due to the saddle-node bifurcation of the neuron model used for the units, with a threshold at (constant) current $I_T = 0.161$ mA/cm^2. Additionally, as a consequence of the bifurcation structure, the processing neuron starts to spike with a very low frequency (formally zero). As the initial frequency is very low, we need to increase J_{EA} in order to get a measurable frequency. As shown in Figure 2a, by increasing J_{IA} the same behavior is found, but curves are shifted towards the right.

This mutual interaction can be observed in Figure 2b, where it is shown the minimum input signal J_{EA} required

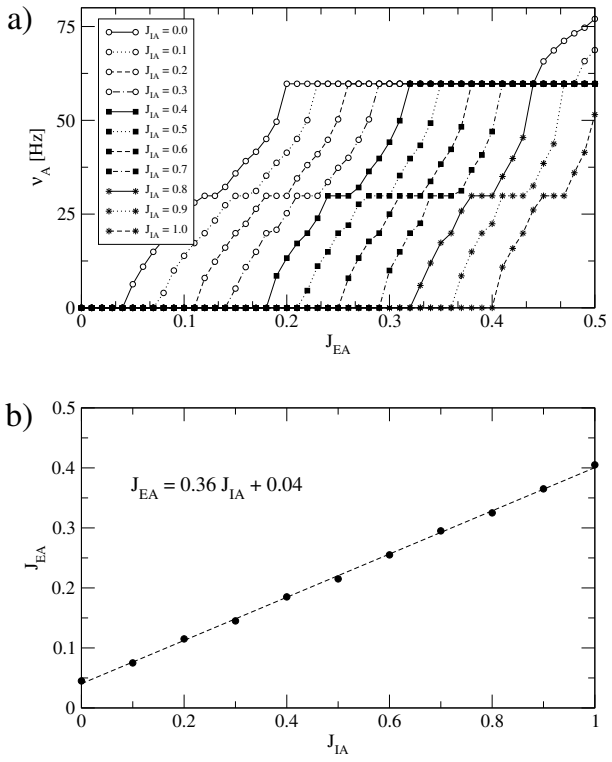

Fig. 2. (a) Mean frequency of the processing neuron as a function of the excitatory input J_{EA}, for different values of a simultaneous inhibitory input J_{IA}. The reference neuron has an input current $I_R = 1$ mA/cm^2, which sets its frequency to $\nu_R \approx 60$ Hz. (b) Minimum value of the signal J_{EA} necessary to produce a measurable response in the processing neuron, as a function of the signal J_{IA}.

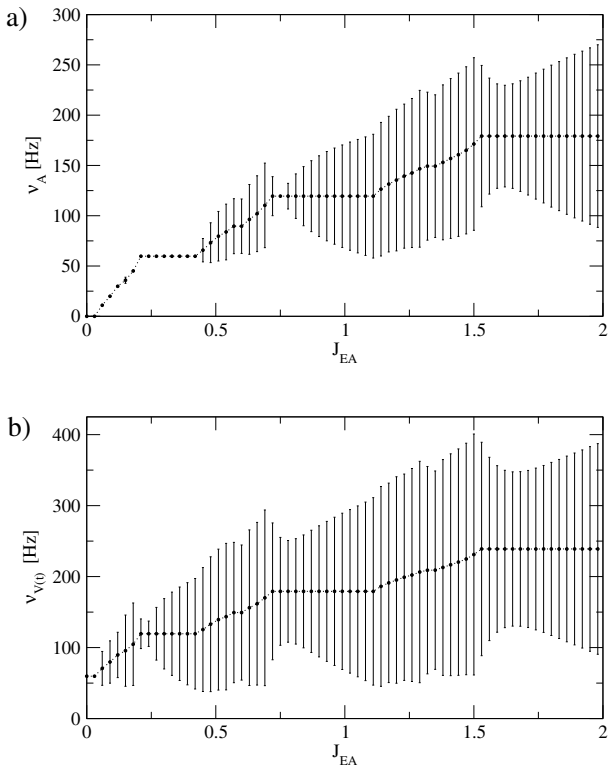

Fig. 3. (a) Frequency ν_A of the processing neuron (mean and dispersion) as a function of the input signal J_{EA} ($J_{IA} = 0$). (b) Frequency $\nu_{V(t)}$ of the compound signal $V(t) = V_R(t) + V_A(t)$ (mean and dispersion) as a function of the input signal J_{EA}. Each point corresponds to a 20 000 ms-long simulation.

to make the processing neuron to fire with a low measurable frequency as a function of the input signal J_{IA}. These J_{EA} values correspond to the threshold of the curves in Figure 2a. Both magnitudes are related by a lineal dependence with slope different from unity, indicating that the excitatory effect is stronger than the inhibitory one ($J_{EA} = 0.36 J_{IA} + 0.04$). Additionally, we observe that for $J_{IA} = 0$, a signal $J_{EA} = 0.04$ is necessary to activate minimally the processing neuron.

This model of two neurons coupled by an axo-axonic mechanism behaves in analogy to a classical perceptron with a sigmoid activation function. In effect, when the input signals J_{EA} and J_{IA} verify that $J_{EA} > 0.36 J_{IA} + 0.04$, the system is set in the upper region in Figure 2b and the processing neuron is activated or "on". In the opposite case, when $J_{EA} < 0.36 J_{IA} + 0.04$ the processing neuron has no activity, so it is "off".

The previous relationship indicates that the effect of the excitatory signal is stronger than the inhibitory one and, therefore, the ratio given by its slope can be used to rescale normalization constants g_E and g_I in equation (3). We take these constant values as $g_E = 0.36$ and $g_I = 1$; this election ensures that the effect of the input signals due to the neural activity of the network is equivalent despite the kind of synapse (excitatory or inhibitory). Additionally, with this definition we simplify the meaning of the weights, since an excitatory and an inhibitory synapse with the same weight values have equivalent but opposite synaptic effects.

Note that the selected neuron model allows us to have a step-like activation function, analogously to the situation we have previously analyzed with phase oscillators (Ref. [16]). In that work, the strenght of the synaptic modulation by the input signals is controlled by a factor α. In particular, we have shown that for $|\alpha| > 1$ the system presents only one stable attractor of the dynamics. On the other hand, the case with $|\alpha| < 1$ corresponds to a system with bistability, similarly to the Hodkgin-Huxley neural model. Clearly, in this last situation, the evolution of the system may depend on the initial conditions, a regime that we do not address in the present study.

3.2 Synchronization properties

Synchronization properties of this system of two neurons are important to understand the information processing in networks constructed with these elements. To this end, we use the system represented in Figure 1a with the set of parameters defined in the previous subsection (Sect. 3.1).

Figure 3a shows the mean frequency of the processing neuron ν_A and its standard deviation as a function of

the input signal J_{EA}, in the absence of inhibition. Mean and standard deviation are calculated from corresponding properties in the set of interspike intervals observed in a fixed temporal window and the inverse relationship that relates both quantities. As shown, there are several plateaus, whether noisy or not, where the processing neuron follows integer multiples of the frequency of the reference neuron ($\nu_R \approx 60$ Hz). This situation corresponds to frequency locking between the neurons. When $0.19 < J_{EA} < 0.45$, the processing neuron has a periodic firing with 1:1 frequency locking and small dispersion. For larger values of J_{EA}, the frequency of the processing neuron can be 1:2 or 1:3 frequency locked to the reference neuron, as shown in Figure 3a. In these cases, the incoming signal is periodic and the dispersion observed arises from the presence of irregular interspike periods in the processing neuron.

In order to study the phase synchronization between the processing and reference neurons, we define a compound signal $V(t) = V_A(t) + V_R(t)$ and measure its mean frequency and dispersion, which are shown in Figure 3b as a function of the excitatory signal J_{EA}. For any value of J_{EA}, firing frequency of the processing neuron presents a large dispersion, except for $J_{EA} \approx 0.225$ where a small deviation is observed. In general, both neurons do not fire simultaneously due to the time course of $s_{ER}(t)$, since there are no instantaneous connections between reference and processing neurons, and this is the cause of the irregularity observed in the interspike periods of $V(t)$.

This irregularity can better appreciated in Figure 4, where we present the histograms $d(T)$ for the interspike intervals of the signal $V(t)$ (left panels) and the individual signals $V_R(t)$ and $V_A(t)$ (right panels), for different representative values of J_{EA}. For $J_{EA} = 0.225$, Figures 4a and 4b, we observe that the interspike interval presents a distribution with two very close peaks (see Fig. 4a). This is clear in Figure 4b where the signals of both neurons are shown. For this input signal both neurons fire at the same frequency but with a phase difference almost half of the period. Since this phase difference is not exactly in the middle, we find two peaks in the histogram. For larger values of J_{EA} and up to $J_{EA} = 0.425$, both neurons still fire at the same frequency, but the phase difference between the signals is steadily reduced; at $J_{EA} = 0.425$ both neurons spike with a small phase difference and, therefore, a large dispersion for the frequency of the compound signal (see Figs. 4c and 4d). A further increase in J_{EA} disrupts the 1:1 frequency locking and the processing neuron increases its own frequency.

A similar situation is found is the second plateau, when the frequency of the processing neuron doubles that of the reference neuron. Figures 4e and 4f account for this situation, as $J_{EA} = 0.75$. In this case, the processing neuron exhibits certain interspike interval and, since frequencies are 1:2 locked, spikes from the reference neuron form two phase differences with previous spikes; therefore, two additional peaks appear in the histogram (see Fig. 4e). As shown in Figure 3a, at $J_{EA} = 0.75$ the dispersion of the compound signal's frequency presents a local

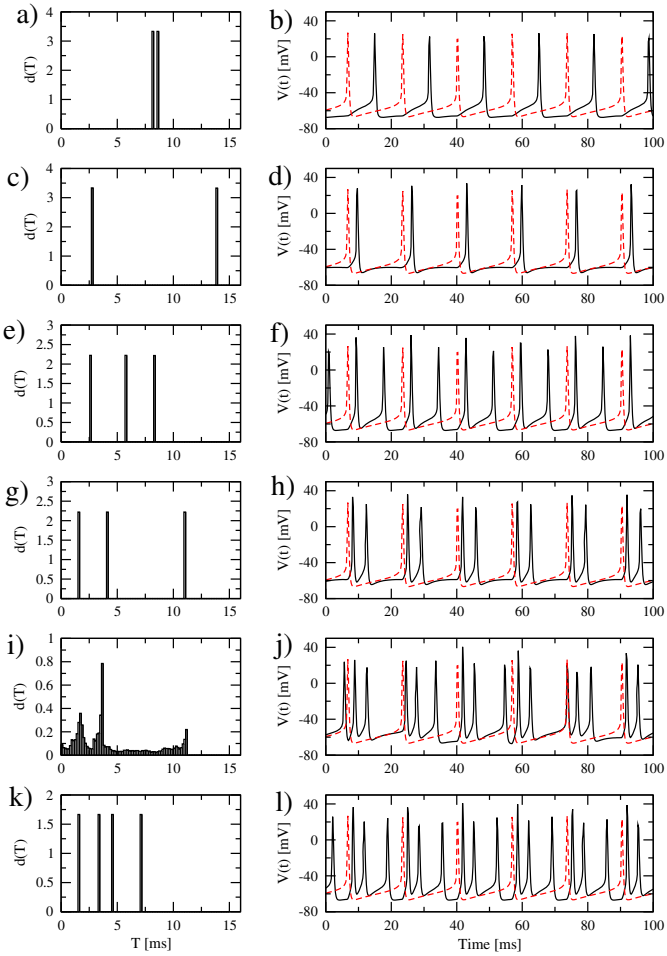

Fig. 4. Left column: histograms of the interspike periods of the potential $V(t) = V_R(t) + V_A(t)$. The histograms are normalized to unity, with binwidth of 0.2 ms. Right column: temporal evolutions of the potentials $V_R(t)$ (reference neuron, dashed red curve) and $V_A(t)$ (processing neuron, black continuous curve). Different rows correspond to different values of input signal J_{EA}: $J_{EA} = 0.225$ (a) and (b), $J_{EA} = 0.425$ (c) and (d), $J_{EA} = 0.750$ (e) and (f), $J_{EA} = 1.10$ (g)–(h), $J_{EA} = 1.45$ (i) and (j), and $J_{EA} = 1.60$ (k) and (l).

minimum. As before, as input external signal increases (up to $J_{EA} = 1.1$), signals still are 1:2 frequency locked, but the first spike of the processing neuron's doublet (per period of the reference neuron spiking) is activated earlier and therefore, it is closer to the spike produced by the reference neuron. Additionally, since external signal is stronger, both spikes of the processing neuron are closer each other. As a consequence, the three peaks in the histogram spread and the frequency becomes noisier (see Figs. 4g and 4h).

A further increase in the external signal J_{EA} sets the system in a non frequency locking regime, as it is shown in Figures 4i and 4j for $J_{EA} = 1.45$. Although there are some clear main frequencies (periods) (see Fig. 4i), the system evolves now in a quasi-periodic fashion. Finally, when the processing neuron has three times the frequency of the reference neuron, they produce a third plateau

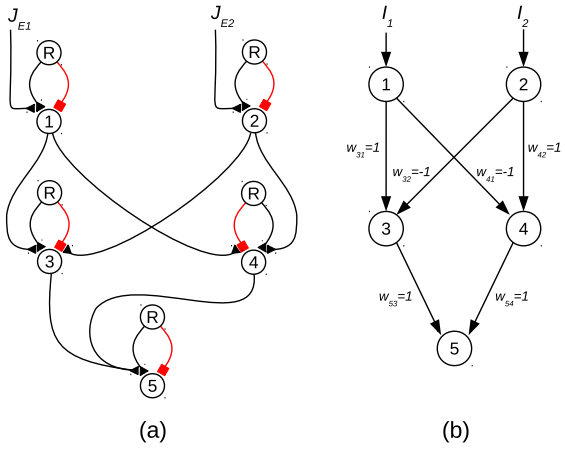

Fig. 5. (a) Network of spiking processing units able to solve the XOR logic problem. All elemental units share a single reference neuron R; for the sake of clarity, we repeated it for each processing unit. (b) Classical feedforward neural network able to solve the same problem. The XOR problem consists of solving the following input-output relationships $[(J_{E1}, J_{E2}) \rightarrow \nu_5]$: ("off", "off") → "off", ("on", "off") → "on", ("off", "on") → "on", and ("on", "on") → "off".

with 1:3 frequency locking and different phase differences, which depends on the input signals J_{EA} (see, for example, Figs. 4k and 4l).

In conclusion, the neurons composing the elemental processing unit develops frequency locking synchronization for different ranges of J_{EA}, where their frequencies are related by integer ratios. As shown, in these regimes, phase differences between both signals depends on J_{EA}. When both signals are not frequency locked, the system behaves in a quasi-periodic, but irregular, way.

3.3 Multilayer feedforward perceptron network

In this subsection, we construct an explicit example of a multilayer feedforward network using our previously designed processing units. The system shown in Figure 5a is the equivalent to a classical system, shown in Figure 5b, capable to solve the XOR problem by the proper set of weights $\{w\}$ [35], which play the role of an adjacency matrix of the network. In order to translate this classical system to our model, we construct the set of inhibitory weights $\{w^I\}$ from those negative weights $\{w{:}w < 0\}$ in the classical model (where w^I is the absolute value of w), and the set of excitatory weights $\{w^E\}$ from the corresponding positive weights $\{w{:}w > 0\}$. With these two sets of connections we link our processing units as equation (3) indicates. An excitatory weight w^E_{ij} connects the output of the processing unit n_j to the excitatory input of the processing unit n_i. Conversely, an inhibitory weight w^I_{ij} connects the output of the processing unit n_j to the inhibitory input of the processing unit n_i (compare both networks in Fig. 5). Finally, a processing unit n_i in the first layer only can have an input external signal J_{Ei} different from zero (external drive is always positive; therefore, signal J_{Ii} is zero), without inputs from other units. In our architecture, all the processing units have the same reference neuron R.

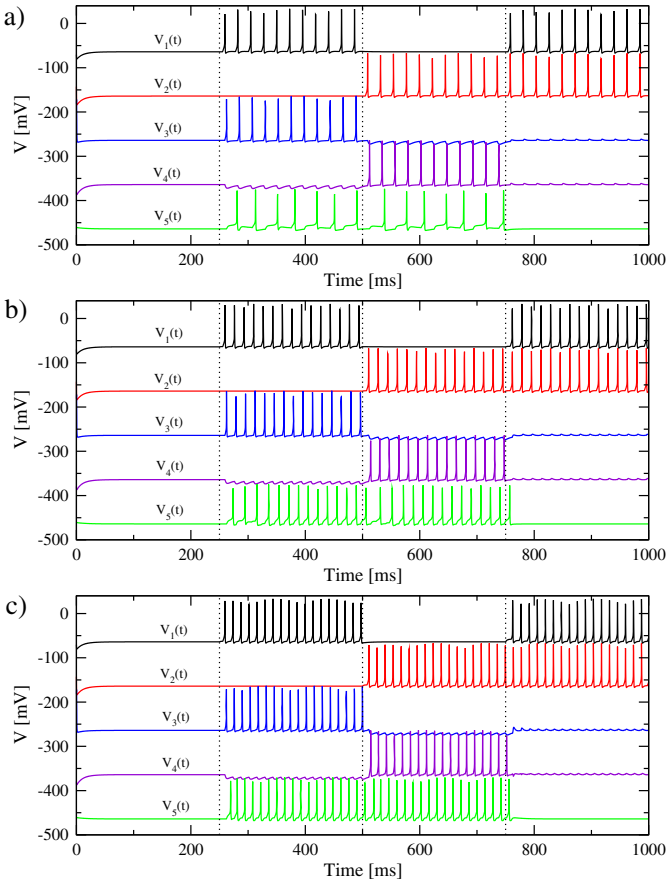

Fig. 6. The XOR problem resolution in action. Potentials of the neurons as function of time. Potentials have been shifted according to $V_i(t) = V_i(t) + 100(i-1)$ in order to improve visualization. The frequency of the reference neuron is $\nu_R \approx 44.1$ Hz ($i_R = 0.7$ mA/cm^2) (a), $\nu_R \approx 59.7$ Hz ($i_R = 1.0$ mA/cm^2) (b), $\nu_R \approx 71.4$ Hz ($i_R = 1.25$ mA/cm^2) (c). System parameters are $g_E = 0.36$, $g_I = 1$, $W = 20$, and $J_{Ii} = 0$. The external input signals are $J_{E1} = 0$ and $J_{E2} = 0$ for $0 < t < 250$ ms, $J_{E1} = 0.35$ and $J_{E2} = 0$ for $250 < t < 500$ ms, $J_{E1} = 0$ and $J_{E2} = 0.35$ for $500 < t < 750$ ms, and $J_{E1} = 0.35$ and $J_{E2} = 0.35$ for $750 < t < 1000$ ms. Dotted vertical black lines show these intervals.

In Figure 6 we present the temporal evolutions of the potentials of the neurons composing the network shown in Figure 5a. To demonstrate the ability of the system to operate at different frequencies, we have used three different values of I_R to stimulate the reference neuron. In order to span all possible combinations of logic inputs, we have changed input signals each 250 ms during a 1000 ms-period. The XOR problem consists of solving the following input-output relationships $[(J_{E1}, J_{E2}) \rightarrow \nu_5]$: ("off", "off") → "off", ("on", "off") → "on", ("off", "on") → "on", and ("on", "on") → "off".

During the first 250 ms, both input external signals are zero ($J_{E1} = J_{E2} = 0$) and therefore, all neurons in the network are silent. Between 250 ms and 500 ms, we

set $J_{E1} = 0.35$ and $J_{E2} = 0$; under this input configuration, only neurons n_1, n_3 and n_5 spike. Between 500 ms and 750 ms the symmetric situation is presented, $J_{E1} = 0$ and $J_{E2} = 0.35$, and, correspondingly, neurons n_2, n_4 and n_5 are activated. The most interesting situation appears during the last 250 ms, when both external input signals are active, $J_{E1} = 0.35$ and $J_{E2} = 0.35$. Now both neurons in the first layer present activities, which are cancelled each other out in downstream neurons n_3 and n_4; consequently, output neuron n_5 does not spike. The proper resolution of the XOR problem for three different frequencies of the reference neuron exemplifies the robustness of proposed model (see Figs. 6a–6c), since information is encoded in a binary scheme just as the activity state of the neurons.

3.4 Network operation with different reference frequencies and noise

In the previous subsection, we have seen that the processing neurons can work properly with different frequencies of the reference neuron. Following, we conduct a more extensive study regarding the sensitivity of the network operation with respect to this parameter and analyze the effects of noise applied to neuron potentials. As a prototypic network, we consider the system shown in Figure 5a.

In Figure 7 we present the frequency of the processing neurons ν_i as a function of the frequency ν_R of the reference neuron ($i = 1, \ldots, 5$). In this first study, we do not consider noise effects and dispersion in frequency data arises exclusively from irregular interspike intervals. We study two logic cases, $(J_{E1}, J_{E2}) = (0.35, 0)$ and $(J_{E1}, J_{E2}) = (0.35, 0.35)$, since the other two ones are either uninteresting because of the absence of any dynamical feature, $(J_{E1}, J_{E2}) = (0, 0)$, or do not represent a new configuration, $(J_{E1}, J_{E2}) = (0, 0.35)$. Figure 7 reports only results regarding the first case, because for the case $(J_{E1}, J_{E2}) = (0.35, 0.35)$ the cancellation of activity in downstream neurons does not give any interesting picture.

In Figure 7a we observe that the neuron n_1 in the first layer spikes always with the same frequency as the reference neuron, and neuron n_2 does not spike at all since $J_{E2} = 0$. In the second layer (see Fig. 7b), the neuron n_3 can follow precisely the frequency of the reference neuron up to $\nu_R \approx 86$ Hz. Note that below this point the dispersion is zero, indicating that both reference and processing neurons are frequency locked. For higher values, processing frequency increases more than linearly with respect to the frequency of the reference neuron; also, dispersion in the interspike intervals indicates that the frequency locking state cannot be maintained. Finally, in Figure 7c we show the frequency of the output neuron n_5. This neuron follows initially the reference frequency up to $\nu_R \approx 14$ Hz; after that, a small dip in the linear relationship is observed up to $\nu_R \approx 64$ Hz, when it recovers again the tight locking to ν_R. For higher values, n_5 maintains 1:1 frequency locking to the reference neuron up to $\nu_R \approx 80$ Hz; from then

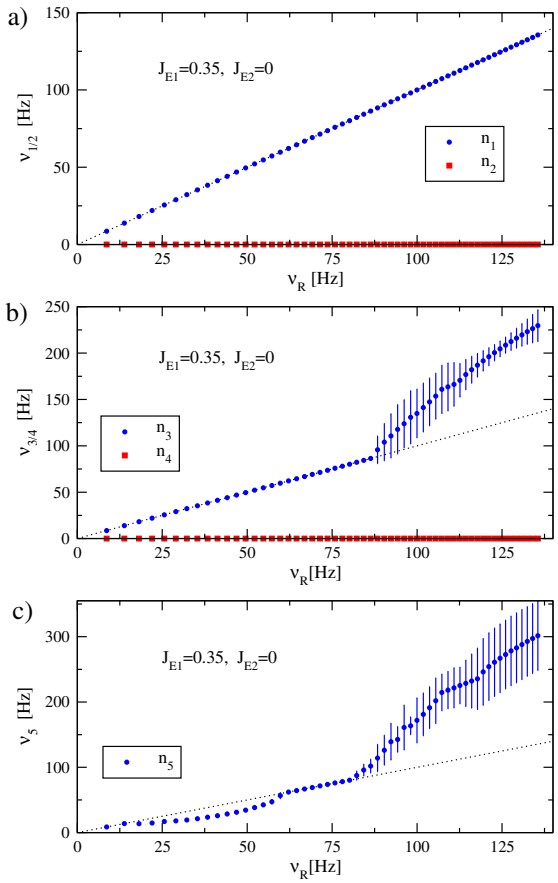

Fig. 7. XOR network operation for different reference frequencies. Frequencies ν_i of the processing neurons as a function of the frequency ν_R of the reference neuron, for the input configuration $J_{E1} = 0.35$ and $J_{E2} = 0$. (a) Frequencies ν_1 and ν_2 for neurons in the first layer. (b) Frequencies ν_3 and ν_4 for neurons in the second layer. (c) Frequency ν_5 of the output neuron. Each point corresponds to frequency data obtained from the interspike intervals collected on a 4000 ms temporal window, after a 1000 ms transient.

on, frequency ν_5 behaves similarly to ν_3, with a supralinear increase with respect to ν_R and the development of irregular interspike intervals. In the second case (not shown), defined by $J_{E1} = 0.35$ and $J_{E2} = 0.35$, neurons belonging to the second and third layers are not active, indicating that incoming signals to the neurons n_3 and n_4 are compensated, as shown previously (see Fig. 6), for any reference frequency.

Behaviors exhibited across the network in these two meaningful cases show that the system can operate properly for a broad range of reference frequencies. Since we encode the information as the state of activation or rest of the neurons, the dispersion of the interspike intervals of the output neurons and the sub- or supra-linear dependence of the processing frequency with respect to ν_R do not degrade the accurate recognition of the logic values.

As shown in the preceding paragraphs, neurons in the network maintain the desired logic input/output relationships for different frequencies. However, network operation robustness should also be demonstrated under noisy

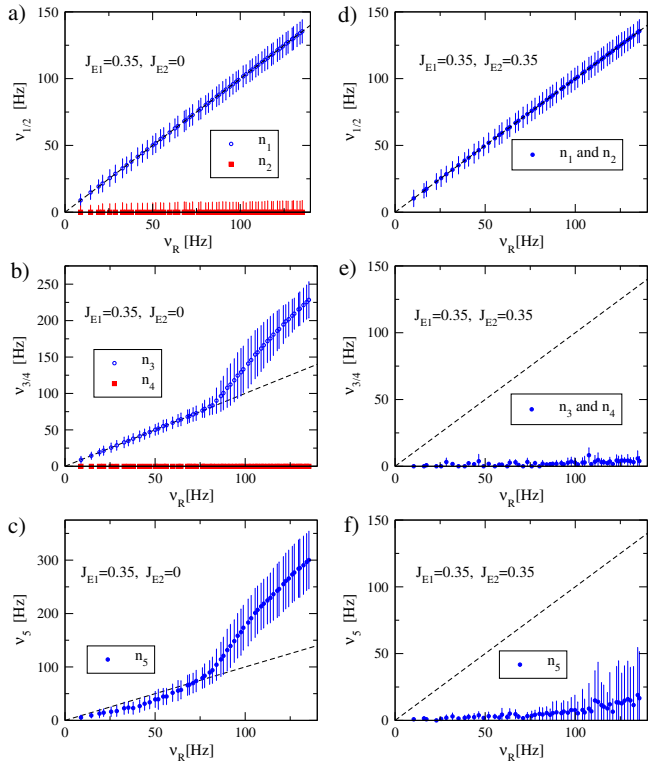

Fig. 8. Frequencies of the neurons composing the XOR-solving network as a function of the reference frequency ν_R, under the effect of noise. (a)–(c) Logic case defined by $J_{E1} = 0.35$ and $J_{E2} = 0$. (d)–(f) Logic case defined by $J_{E1} = 0.35$ and $J_{E2} = 0.35$. Noise intensity is $T = 0.5$.

conditions. To that purpose, we study the effects on the network operations of an independent additive noise applied to input currents. In particular, we have used a Gaussian white noise $\xi_i(t)$, defined by $\langle \xi_i(t) \rangle = 0$ and $\langle \xi_i(t_1)\xi_j(t_2) \rangle = \delta_{ij}\delta(t_1 - t_2)$ $(i, j = 1, \ldots, N)$, added to the input current to neuron V_i and scaled by the noise intensity T (see the Appendix). For these simulations, we have used a stochastic Runge-Kutta algorithm of second order with $\Delta t = 0.01$ as the temporal step.

Similarly to Figures 7 and 8 shows the frequency of the processing neurons as a function of the reference frequency, in noisy conditions. In the left column of Figure 8 (Figs. 8a–8c), we present results for the input combination $J_{E1} = 0.35$ and $J_{E2} = 0$. Even with a small added dispersion, we clearly observe that mean frequencies are the same as in the case without noise (Fig. 7). The smaller dispersion exhibited by neuron n_4 in comparison to n_2 results particularly interesting; this is due to the fact that neuron n_4 has a strong inhibitory input from n_1 and therefore, it maintains a large gap to reach the threshold which discourages spiking. Finally, we observe that noise increases for successive layers, as expected from an accumulative effect.

In the right column of Figure 8 (Figs. 8d–8f), we present results for the last logic case with $J_{E1} = 0.35$ and $J_{E2} = 0.35$. In this situation, we observe that now both input neurons present dispersions on their frequencies due to the noise (both response functions are superimposed in Fig. 8d). As expected for this logic case, neurons in the second layer present activities with a very low frequency, which are driven by their intrinsic noises and the imperfect cancellation of the noisy inputs from the preceding layer (Fig. 8e). Finally, in Figure 8f we observe that the output neuron has a very small processing frequency with a large dispersion, which increases as the frequency of the reference neuron does. This rising of the noise effect with the frequency can be understood by taking into account the effect of the function $s_{ER}(t)$. In effect, when the reference neuron has a high frequency $s_{ER}(t)$ does not decay to zero before a new spike arrives, and this situation generates a continuous baseline that opposes to the cancellation designed by the connections (details about the function $s_{ER}(t)$ are given in the Appendix). In this condition, equation (1) behaves similarly to a normal chemical synapse with a constant weight. Despite this noise effect, it is clear that the activity of the output neuron is much smaller than the reference neuron and, in consequence, we can recognize the logic level properly. In general, we observe that the network can operate with a high level of noise. The main reason for this well-behaved operation is that the natural state of the neurons without input current is far from the threshold needed to excite the neurons, and even afterwards the spiking activity starts with a very low frequency due to the saddle-node bifurcation of the Wang-Buzsáki neuron model.

3.5 Effects of the parameters J_E and W on network processing

The parameter J_E defines the frequency and phase difference between the reference neuron and those neurons in the first layer of the network shown in Figure 5a. Similarly, the parameter W controls frequencies and phase differences between the reference and neurons in downstream layers. Even when, in our binary conception of the processing, only the frequency determines whether the neuron is behaving as logically designed or not, a neuron needs a proper phase difference between the spike of the reference neuron and the presynaptic ones in order to have an active response. Moreover, as shown in Figure 4, spike time phase differences between reference and active neurons depend on couplings (here J_E and W) and are indicative of different regimes; for example, in Figure 4, multi-peaked histograms arise when frequency locking is established. Therefore, it is expected than parameters J_E and W command processing frequency in a non trivial way.

In this subsection, we focus on the frequencies of the processing neurons composing the network illustrated in Figure 5a as a function of the parameters J_E and W for a fixed reference frequency $\nu_R \approx 60$ Hz, in a noise-free scenario. In Figures 9a and 9b, we show the frequencies ν_3 and ν_5 of the corresponding processing neurons for the logic case defined by $J_{E1} = J_E$ (or "on") and $J_{E2} = 0$ (or "off"). The active neuron in the first layer just follows the behavior previously analyzed in Figure 3 and it is not shown here. For neuron n_3, we find a rich structure with

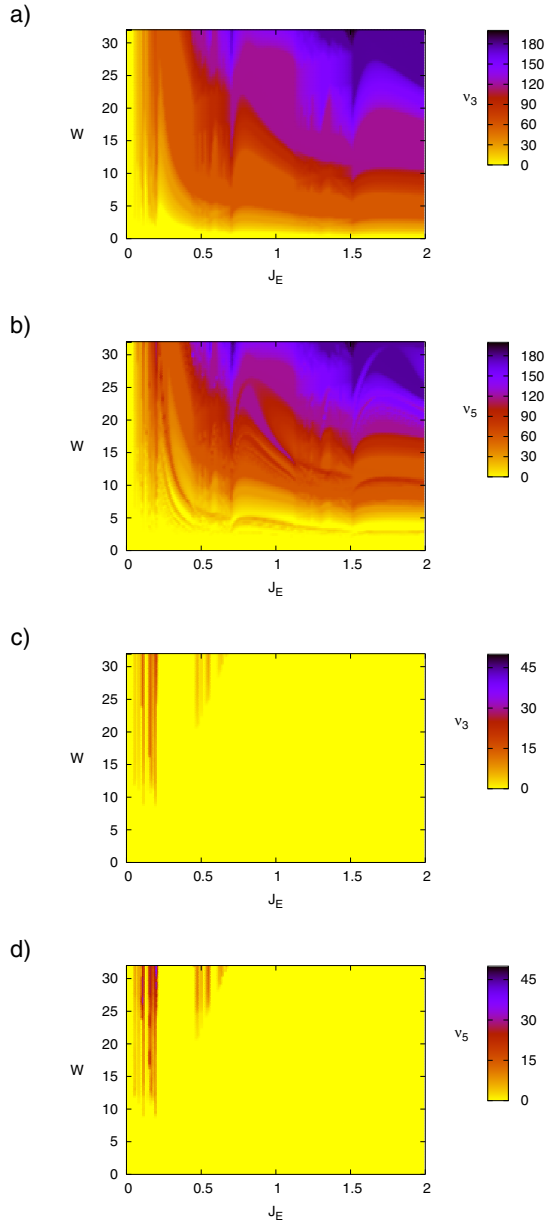

Fig. 9. Frequencies of the processing neurons composing the XOR-solving network as a function of parameters J_E and W. (a) and (b) frequencies ν_3 and ν_5 for the logic case defined by J_{E1} = "on" and J_{E2} = "off". (c) and (d) Frequencies ν_3 and ν_5 for the logic case defined by J_{E1} = "on" and J_{E2} = "on". Reference neuron has a frequency $\nu_R \approx 60$ Hz. Colorbar indicates corresponding frequencies measured in Hz.

plateaus at $\nu_3 = 60$ Hz, $\nu_3 = 120$ Hz and $\nu_3 = 180$ Hz, in different regions of the parameter space (see Fig. 9a). For neuron n_5, the structure is more complex as more neuron responses shape output frequency (see Fig. 9b).

Figures 9c and 9d show equivalent results when both input processing units are activated: $J_{E1} = J_{E2} = J_E$ (or "on"). Satisfying the XOR operation, we observe that, along almost the entire parameter space, cancellation between excitatory and inhibitory synapses work properly and neurons in the second and third layers do not produce spikes. However, there are small regions of J_E and W values where these compensations are not perfectly effective. These regions, where input neurons cannot get frequency locking synchronization to reference neuron, may be roughly delimited by $J_E < 0.2$ and $0.44 < J_E < 0.72$. Obviously, parameters in these regions do not allow to solve properly the XOR problem and must be avoided.

As shown in this subsection, the proposed system is robust as it can work in a broad range of coupling parameters. It is important to note that the network designed here has the particularity that all processing units have the same number of inhibitory and excitatory input connections. This fact allows us to tightly control operation frequencies and may not be the case in more complex networks where the same neuron can have different modulated weight values depending on the logic input signals and then, different values of frequencies.

4 Discussion and conclusions

In this work, we have presented a neural circuit (processing unit) able to work analogously to a classical perceptron. Further, a feedforward network capable to solve the XOR problem was constructed using these units, where underlying connectivity mimics the structure of a classical feedforward XOR-solving network. As shown, we have designed a system that works properly with different processing frequencies and exhibits a marked robustness against noise. The architecture of the processing unit is a realistic implementation of the model of phase oscillators previously analyzed by one of the authors in reference [16]. Although in the previous model the information was encoded as phase differences and now as neuronal activities, it is possible to map them by consistently defining equivalent states; for example, while an active (inactive) state in reference [16] is given by certain fixed point of the dynamics, here it corresponds to a sustained spiking (quiescent) regime. Importantly, both models share hetero-synapsis as a key mechanism to process logic states and gate information flow according to external inputs or other neuron's activity.

A previous model of a spiking feedforward neural network proposed by Bohte et al. [17] has demonstrated that learning classification tasks by backpropagating errors can be achieved with threshold neurons and a relatively realistic synaptic dynamics. The main difference between this model and our work is the way to encode information. Whereas in Bohte model the information is encoded by the interspike intervals as a time series, in our model the information is given as the neural activity. Furthermore, our model can be used consecutively to a classical perceptron feedforward model, which is used to learn a particular task with standard methods (e.g. backpropagating errors over perceptrons). Once a network topology is so defined, its translation to our spiking perceptron model by appropriately connecting processing units is straightforward. In general, we can indicate that both models are complementary to each other.

The model presented in this work is able to operate properly in a broad range of system parameters. This fact allows us to easily translate the network structure from the classical model to the spiking perceptron. As shown, it is not necessary a significant effort to finely tune parameters W and J_E. Additionally, the fact that the system can work with different references frequencies ν_R allows the system to solve the same logic problem with different operation regimes and, obviously, meaningful information can also be encoded by this operation frequency. For example, solving the XOR problem at 50 Hz can have a very different meaning from an equivalent operation at 90 Hz.

As demonstrated, the spiking perceptron is markedly robust against noise. The main reason for this behavior is the fact that neurons are in a state far from the bifurcation point; thus, noise must overcome a large gap to threshold to activate neurons. Additionally, the onset to spiking for neurons in this model is given with limit circles of arbitrary low firing rates, so the proper classification as an "activated" state has to be associated to a large input current. The second important fact is that a neuron needs particular correlations between the presynaptic (to the axo-axonic connection) and reference neurons in order to activate a neuron, due to the time course of the postsynaptic effects given by the signals $s_{\alpha i}(t)$. Thus, the spontaneous spike of a presynaptic neuron cannot be processed if the reference neuron does not trigger the corresponding synapse. That is true for relatively low frequencies ν_R; for larger values of ν_R, the function $s_{ER}(t)$ can generate a significant baseline that continuously drives membrane potential close to the threshold and the forced synchronization is lost.

Appendix: Neural and synaptic models

A.1 Neurons

All neurons evolve according to the Wang-Buzsáki neuron model [20]; in detail, dynamics is given by the following set of equations

$$C\frac{dV}{dt} = I_{syn} + g_{Na}m_\infty^3(V)h(V_{Na}-V) + g_K n^4(V_K - V) + g_L(V_L - V) + T\xi(t), \tag{A.1}$$

$$\frac{dh}{dt} = \frac{h_\infty(V)-h}{\tau_h(V)}, \tag{A.2}$$

$$\frac{dn}{dt} = \frac{n_\infty(V)-n}{\tau_n(V)}, \tag{A.3}$$

where V is the membrane potential, h is the inactivating gate of sodium channels, and n is the activating subunit of potasium channels. The constant T defines noise intensity and $\xi(t)$ represents a Gaussian white noise of unitary variance. Functions $m_\infty(V)$, $h_\infty(V)$ and $n_\infty(V)$, and the characteristic times $\tau_h(V)$ and $\tau_n(V)$ are given by $x_\infty(V) = a_x/(a_x+b_x)$, $\tau_x = 1/(a_x+b_x)$ with $x = m, n, h$. Particular values are:

$$a_m = \frac{-0.1(V+35)}{\exp(-0.1(V+35))-1}, \tag{A.4}$$

$$b_m = 4\exp(-(V+60)/18), \tag{A.5}$$

$$a_h = 0.35\exp(-(V+58)/20), \tag{A.6}$$

$$b_h = \frac{5}{\exp(-0.1(V+28))+1}, \tag{A.7}$$

$$a_n = \frac{-0.05(V+34)}{\exp(-0.1(V+34))-1}, \tag{A.8}$$

$$b_n = 0.625\exp(-(V+44)/80). \tag{A.9}$$

Time constants are expressed in milliseconds. Numerical values of the parameters are: $g_{Na} = 35$ mS/cm^2, $g_K = 9$ mS/cm^2, $g_l = 0.1$ mS/cm^2, $V_{Na} = 55$ mV, $V_K = -90$ mV, $V_l = -65$ mV and $C = 1$ μF/cm^2.

A.2 Synapses

Synaptic input current to a neuron, I_{syn}, is modelled according to equation (1). Numerical values of excitatory and inhibitory reverse potentials are $V_E = 0$ mV and $V_I = -80$ mV. Following Hansel and Mato [22], here we describe the phenomenological function $s_{\beta i}(t)$ that models the dynamical evolution of a synaptic contact. Following a spike of a presynaptic neuron I at $t = 0$, post-synaptic interactions (synaptic processes) are modelled by

$$f_{\beta i}(t) = \frac{1}{\tau_{1\beta}-\tau_{2\beta}}\left[\exp\left(-\frac{t}{\tau_{1\beta}}\right) - \exp\left(-\frac{t}{\tau_{2\beta}}\right)\right]\Theta(t). \tag{A.10}$$

The subindex β can be E or I, depending on the kind of synapse (excitatory or inhibitory, respectively). The interaction process is governed by two characteristic times $\tau_{1\beta}$ (rise phase) and $\tau_{2\beta}$ (decay phase). Their numerical values are $\tau_{1E} = 1$ ms, $\tau_{2E} = 3$ ms, $\tau_{1I} = 1$ ms and $\tau_{2I} = 6$ ms. $\Theta(t)$ is the Heaviside function.

The neuron I produces spikes at times t_i^{spikes}. The total accumulated effect of these spikes on a given post-synaptic evolution $s_{\beta i}(t)$ is given by:

$$s_{\beta i}(t) = \sum_{\text{spikes}} f_{\beta i}(t - t_i^{\text{spikes}}). \tag{A.11}$$

Numerically, we compute the function $s_{\beta i}(t)$ by defining two new variables as follows:

$$\dot{\epsilon}_{1\beta i} = -\frac{\epsilon_{1\beta i}}{\tau_{1\beta}} + \sum_{\text{spikes}} \delta(t - t_i^{\text{spikes}}), \tag{A.12}$$

$$\dot{\epsilon}_{2\beta i} = -\frac{\epsilon_{2\beta i}}{\tau_{2\beta}} + \sum_{\text{spikes}} \delta(t - t_i^{\text{spikes}}). \tag{A.13}$$

Then, the function $s_{\beta i}(t)$ is given by:

$$s_{\beta i}(t) = \frac{1}{\tau_{1\beta} - \tau_{2\beta}}(\epsilon_{1\beta i} - \epsilon_{2\beta i}). \quad \text{(A.14)}$$

When a neuron spikes periodically its function $s_{\beta j}(t)$ takes a simple form. Let's consider that a neuron j with a post-synaptic effect β and interspike period T has fired its last spike at time $t = 0$. Then, the function $s_{\beta j}(t)$ between $t = 0$ and $t = T$ (following spike) reads

$$s_{\beta j}(t) = \sum_{n=0}^{\infty} f_{\beta j}(t + Tn). \quad \text{(A.15)}$$

In this expression we add the effects of previous spikes at times $-Tn$, where n is the spike index. Taking into account the expression of the function $f_{\beta j}(t)$ in equation (A.10), we can write

$$s_{\beta j}(t) = \frac{1}{\tau_{1\beta} - \tau_{2\beta}} \left[\frac{e^{-t/\tau_{1\beta}}}{1 - e^{-T/\tau_{1\beta}}} - \frac{e^{-t/\tau_{2\beta}}}{1 - e^{-T/\tau_{2\beta}}} \right]. \quad \text{(A.16)}$$

We observe that $s_{\beta j}(0)$ is equal to $s_{\beta j}(T)$; that is, the function is periodic with period T. Additionally, the mean value in a period is $\nu_{\beta j}$, the frequency of the neuron j:

$$\langle s_{\beta j}(t) \rangle = \frac{1}{T} = \nu_{\beta j}. \quad \text{(A.17)}$$

References

1. F. Rosenblatt, *Principles of Neurodynamics: Perceptrons and the Theory of Brain Mechanisms* (Spartan Books, Washington, 1962)
2. D.E. Rumelhart, G.E. Hinton, R.J. Williams, Nature **323**, 533 (1986)
3. J.J. Hopfield, Proc. Natl. Acad. Sci. USA **79**, 2554 (1982)
4. J. Hertz, A. Krogh, R.G. Palmer, *Introduction to the Theory of Neural Computation* (Addison-Wesley, New York, 1991)
5. A.L. Hodgkin, A.F. Huxley, J. Physiol. **117**, 500 (1952)
6. X.-J. Wang, Physiol. Rev. **90**, 1195 (2010)
7. M. Bartos, I. Vida, P. Jonas, Nat. Rev. Neurosci. **8**, 45 (2007)
8. R. Krahe, F. Gabbiani, Nat. Rev. Neurosci. **5**, 13 (2004)
9. B.P. Bean, Nat. Rev. Neurosci. **8**, 451 (2007)
10. W. Maass, Neural Networks **10**, 1659 (1997)
11. Y. Kuramoto, *Chemical Oscillations, Waves, Turbulence* (Springer, New York, 1984)
12. T. Aoyagi, Phys. Rev. Lett. **74**, 4075 (1995)
13. T. Aonishi, K. Kurata, M. Okada, Phys. Rev. Lett. **82**, 2800 (1999)
14. T. Nishikawa, Y.-C. Lai, F.C. Hoppensteadt, Phys. Rev. Lett. **92**, 108101 (2004)
15. P. Kaluza, T. Cioaca, Neurocomputing **97**, 115 (2012)
16. P. Kaluza, Neurocomputing **118**, 127 (2013)
17. S.M. Bohte, J.N. Kok, H. La Poutré, Neurocomputing **48**, 17 (2002)
18. P. D'Souza, S.-C. Liu, R.H.R. Hahnloser, Proc. Natl. Acad. Sci. USA **107**, 4722 (2010)
19. L. Serrano, Mol. Syst. Biol. **3**, 158 (2007)
20. X.-J. Wang, G. Buzsáki, J. Neurosci. **16**, 6402 (1996)
21. J.A. White, C.C. Chow, J. Ritt, C. Soto-Treviño, N. Kopell, J. Comput. Neurosci. **5**, 5 (1998)
22. D. Hansel, G. Mato, Neural Comput. **15**, 1 (2003)
23. J.A. White, M.I. Banks, R.A. Pearce, N.J. Kopell, Proc. Natl. Acad. Sci. USA **97**, 8128 (2000)
24. P.H.E. Tiesinga, J.-M. Fellous, J.V. José, T.J. Sejnowski, Hippocampus **11**, 251 (2001)
25. P.H.E. Tiesinga, T.J. Sejnowski, Neural Comput. **16**, 251 (2004)
26. P.H. Tiesinga, J.-M. Fellous, E. Salinas, J.V. José, T.J. Sejnowski, J. Physiol. **98**, 296 (2004)
27. G. Mato, I. Samengo, Neural Comput. **20**, 2418 (2008)
28. A.B. MacDermott, L.W. Role, S.A. Siegelbaum, Ann. Rev. Neurosci. **22**, 443 (1999)
29. C.H. Bailey, M. Giustetto, Y.-Y. Huang, R.D. Hawkins, E.R. Kandel, Nat. Rev. Neurosci. **1**, 11 (2000)
30. A.J. Cochilla, S. Alford, J. Neurosci. **19**, 193 (1999)
31. D. Schmitz, S. Schuchmann, A. Fisahn, A. Draguhn, E.H. Buhl, E. Petrasch-Parwez, R. Dermietzel, U. Heinemann, R.D. Traub, Neuron **31**, 831 (2001)
32. B. Lamotte D'Incamps, C. Meunier, M.-L. Monnet, L. Jami, D. Zytnicki, J. Comput. Neurosci. **5**, 141 (1998)
33. P. Peretto, J.J. Niez, Biol. Cybern. **54**, 53 (1986)
34. J.J. Arenzon, R.M.C. de Almeida, Phys. Rev. E **48**, 4060 (1993)
35. R. Rojas, *Neural Networks – A Systematic Introduction* (Springer-Verlag, Berlin, 1996)